PERGAMON

Journal of Structural Geology 21 (1999) 493–509

JOURNAL OF STRUCTURAL GEOLOGY

Selective reverse-reactivation of normal faults, and deformation around reverse-reactivated faults in the Mesozoic of the Somerset coast

P.G. Kelly[a,*,1], D.C.P. Peacock[b], D.J. Sanderson[a,2], A.C. McGurk[b]

[a]*Geomechanics Research Group, School of Ocean and Earth Science, University of Southampton, Southampton Oceanography Centre, Southampton SO14 3ZH, UK*

[b]*Rock Deformation Research Group, School of Earth Sciences, University of Leeds, Leeds LS2 9JT, UK*

Received 5 May 1998; accepted 27 January 1999

Abstract

Normal faults exposed in the Triassic–Jurassic limestones and shales of the Somerset coast were formed during the Mesozoic development of the Bristol Channel Basin. Reverse-reactivation of some of these normal faults occurred during Late Cretaceous to Early Tertiary north–south contraction. The contraction is also evident from thrusts and conjugate strike-slip faults. Preferential reactivation of the normal faults is attributed to: (1) decreased fault-plane friction, (2) domino block rotation, (3) displacement magnitude, and (4) fault connectivity. The geometries of overlapping and underlapping zones in reactivated fault zones are dependent on the existing structural geometry. Two distinctive styles of displacement accommodation occur between reverse-reactivated normal faults: (1) formation of a network of strike-slip faults, conjugate about NNE–SSW, and (2) oblique steeply-dipping reverse faults. Interaction between strike-slip and an existing fault is dependent on whether the normal fault was reactivated. The range of structures related to the north–south contraction has been incorporated into a single deformation model, controlled by the northwards movement of the hanging wall of the Quantock's Head Fault. Pure dip-slip movement occurred in the centre of its curved fault trace, with a sinistral component at the western tip, and a dextral component of displacement and strike-slip block rotations occurred at the eastern tip. Shortening of these blocks was achieved through development of a strike-slip fault network and NW-striking thrusts. In an underlap zone, loading of the footwall by the hanging wall block modified the local stress system to allow formation of oblique, steeply-dipping reverse faults.

1. Introduction

Recent discussion of fault reactivation appears to have concentrated on the relationships between fault geometries (e.g. Cooper and Williams, 1989; Dart et al., 1995), orientations of the fault plane to the stress axes (e.g. Sibson, 1985; Huyghe and Mugnier, 1992) and the role of pore fluids (e.g. Sibson, 1995). Gently dipping normal faults, or steeply dipping reverse faults may reflect a diverse fault history. For example, gently dipping normal faults have been shown to develop through normal reactivation of thrusts (Brewer and Smythe, 1984; Enfield and Coward, 1987), and reverse faults with steep dips may reflect a normal fault origin (e.g. Williams et al., 1989).

This paper is based on field observations of faults in the Mesozoic sediments of the Somerset coast in the

* Corresponding author.

E-mail address: p.kelly@OPENMAIL2.VEDB74.sukepabe.simis.com (P.G. Kelly)

[1] Current address: Shell UK Exploration and Production, Seafield House, Hill of Rubislaw, Aberdeen AB15 6GZ, UK

[2] Current address: T.H. Huxley School of Environment, Earth Sciences and Engineering, Royal School of Mines, Imperial College of Science, Technology and Medicine, Prince Consort Road, London SW7 2BP, UK

0191-8141/99/$ - see front matter
PII: S0191-8141(99)00041-3

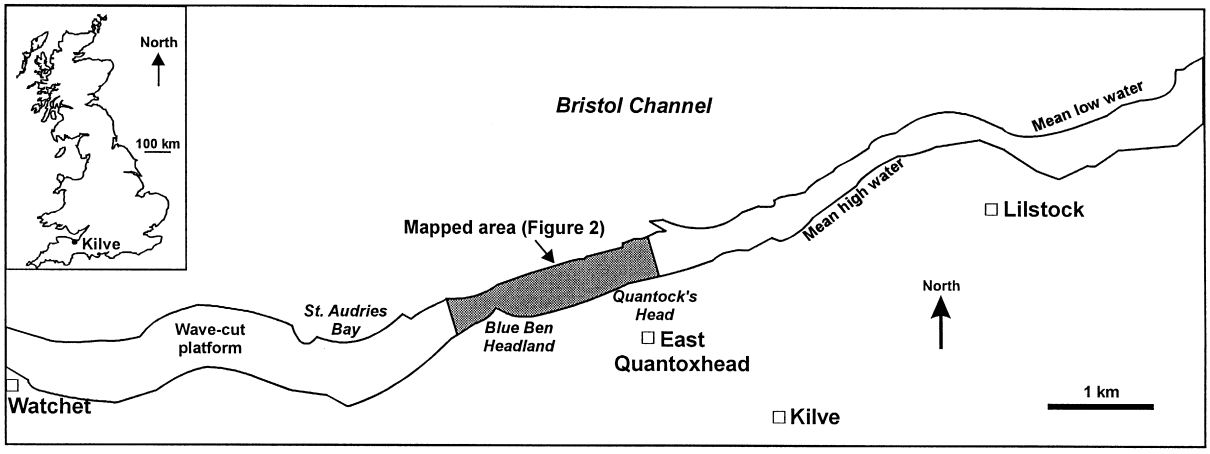

Fig. 1. Map of the foreshore of part of the north Somerset Coast to show the location of Fig. 2, and (inset) map of Great Britain to show the location of the field area.

East Quantoxhead area (Fig. 1). The foreshore and cliff exposures have provided an ideal opportunity to study reverse-reactivated normal faults (Fig. 2) and provide further understanding of similar structures that are often observed on seismic sections, e.g. in the Southern North Sea (Badley et al., 1989), offshore of the British Isles (Roberts, 1989) and the East Shetland Basin (Thomas and Coward, 1995). Recent work on the Bristol Channel Basin has included field-based studies by McLachlan (1986), Peacock and Sanderson (1991, 1992, 1994a), Dart et al. (1995) and Nemcok et al. (1995), and seismic studies by Brooks et al. (1988) and Van Hoorn (1987).

Faults were mapped using a series of ~1:500 scale aerial photographs as a basemap. The high resolution and quality of the aerial photographs enabled individual beds and fault offsets to be traced. Cross-sections through individual fault zones were mapped onto photographs of the cliffs.

This paper begins with an introduction to the geology of the Somerset coast, followed by descriptions of the fault properties. Four models for the preferential reverse-reactivation of the normal faults are discussed, and the geometries of underlapping and overlapping zones are used to develop a model for the contractional deformation at this locality. It is shown that reverse-reactivation of normal faults is strongly influenced by the size of the fault, and several geometric and mechanical reasons for this are given. The preferential reversal of some of the normal faults has led to three distinct styles of overlap zones in map view.

2. Geological setting

The development of the Bristol Channel Basin is believed to have been controlled by the formation of a southward dipping normal fault which is thought to detach onto a major Variscan thrust at depth (Brooks et al., 1988), and was reactivated during the Late Jurassic to the Cretaceous (Van Hoorn, 1987; Lake and Karner, 1987; Dart et al., 1995; Nemcok et al., 1995). The onshore sedimentary sequence consists of Triassic marls and Jurassic limestones, shales and marls (Fig. 2) (Whittaker and Green, 1983). The stratigraphy of the Upper Triassic and Lower Liassic sediments used in this study is based on the divisions of Palmer (1972) as the descriptive names are more applicable to this study. The Kilve Shales and St. Audrie's Shales consist of thin (<0.15 m) limestones interbedded with shales and mudstones up to 3 m thick. The Blue Lias and the Quantock's Beds are also limestone/shale interbeds, but the limestone units are up to 0.6 m thick, and the shales are less than 2 m thick. These Mesozoic sedimentary rocks contain E–W-trending normal faults (e.g. Peacock and Sanderson, 1991, 1992; Bowyer and Kelly, 1995).

A phase of contraction in the Tertiary (Van Hoorn, 1987; Brooks et al., 1988; Chadwick, 1993; Dart et al., 1995; Nemcok et al., 1995) is evident from a seismic study by Van Hoorn (1987) and field exposures of reverse-reactivated normal faults (McLachlan, 1986; Peacock and Sanderson, 1992) and thrusts. Strike-slip faults are conjugate about N20°E (Fig. 3) (Peacock and Sanderson, 1992). Field evidence for the reverse-reactivation of individual normal faults includes thrusts in their hanging walls, kink bands and crenulation cleavage (Peacock and Sanderson, 1992), hanging wall buttress anticlines (Dart et al., 1995), multiple sets of slickenside lineations on a fault plane, and drag of beds. Within a fault zone, individual faults frequently retain finite normal displacements, but are associated with contractional features and strike-slip faults, and occasionally pass laterally into reverse faults. In the Triassic marls at Watchet (Fig. 1), moderately-dipping

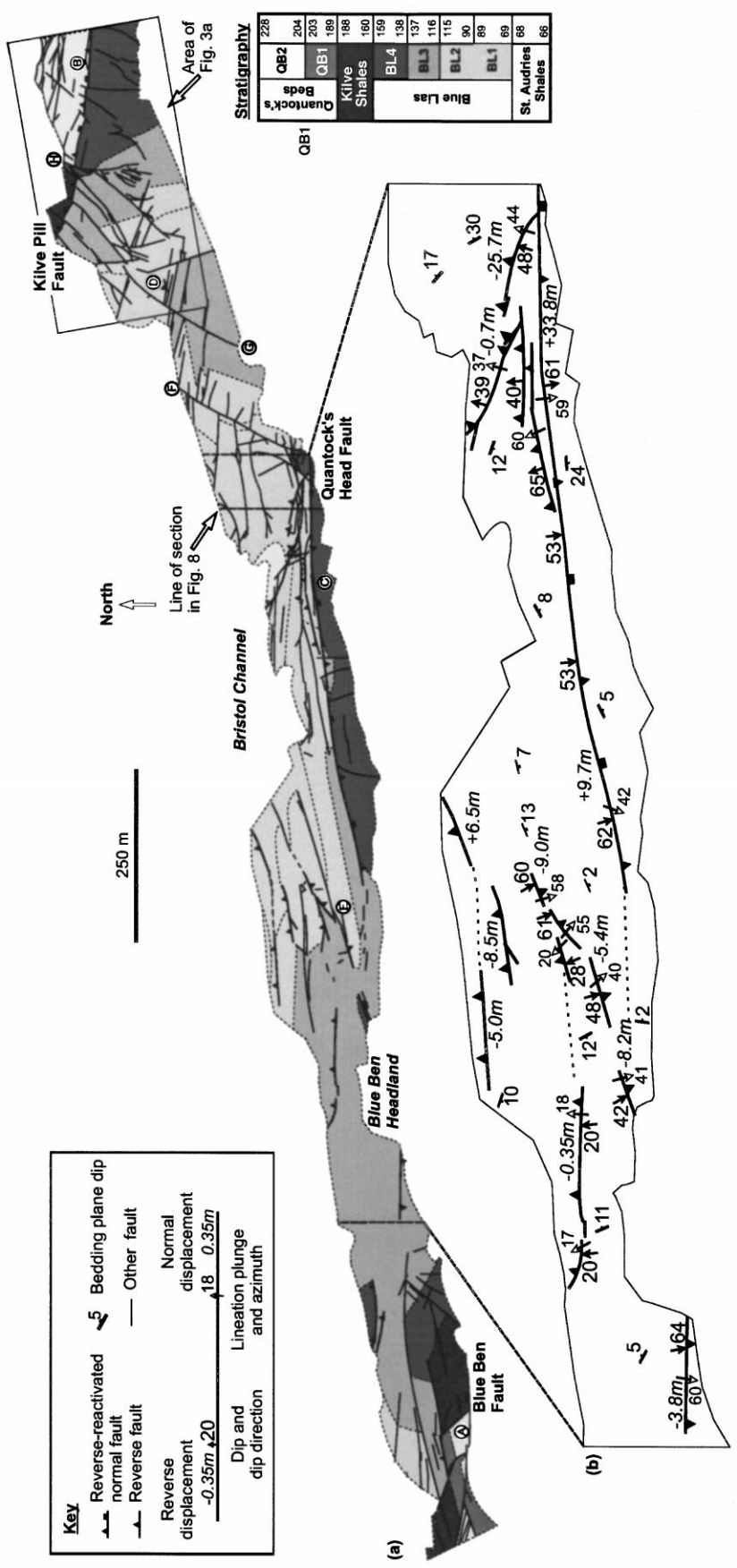

Fig. 2. (a) Map of the faults between East Quantoxhead and St. Audrie's Bay. The bold lines represent the reverse and reverse-reactivated normal faults, and the ticks are on the hanging walls of the faults. All other faults are represented by thin lines. The Blue Lias and Quantock's Beds have been further divided into approximately equal thickness units of 10 m. The lettered locations are referred to in the text. (b) Fault data and copy of part of the map in (a), with unreactivated normal and strike-slip faults removed for clarity. A stratigraphic column is also included.

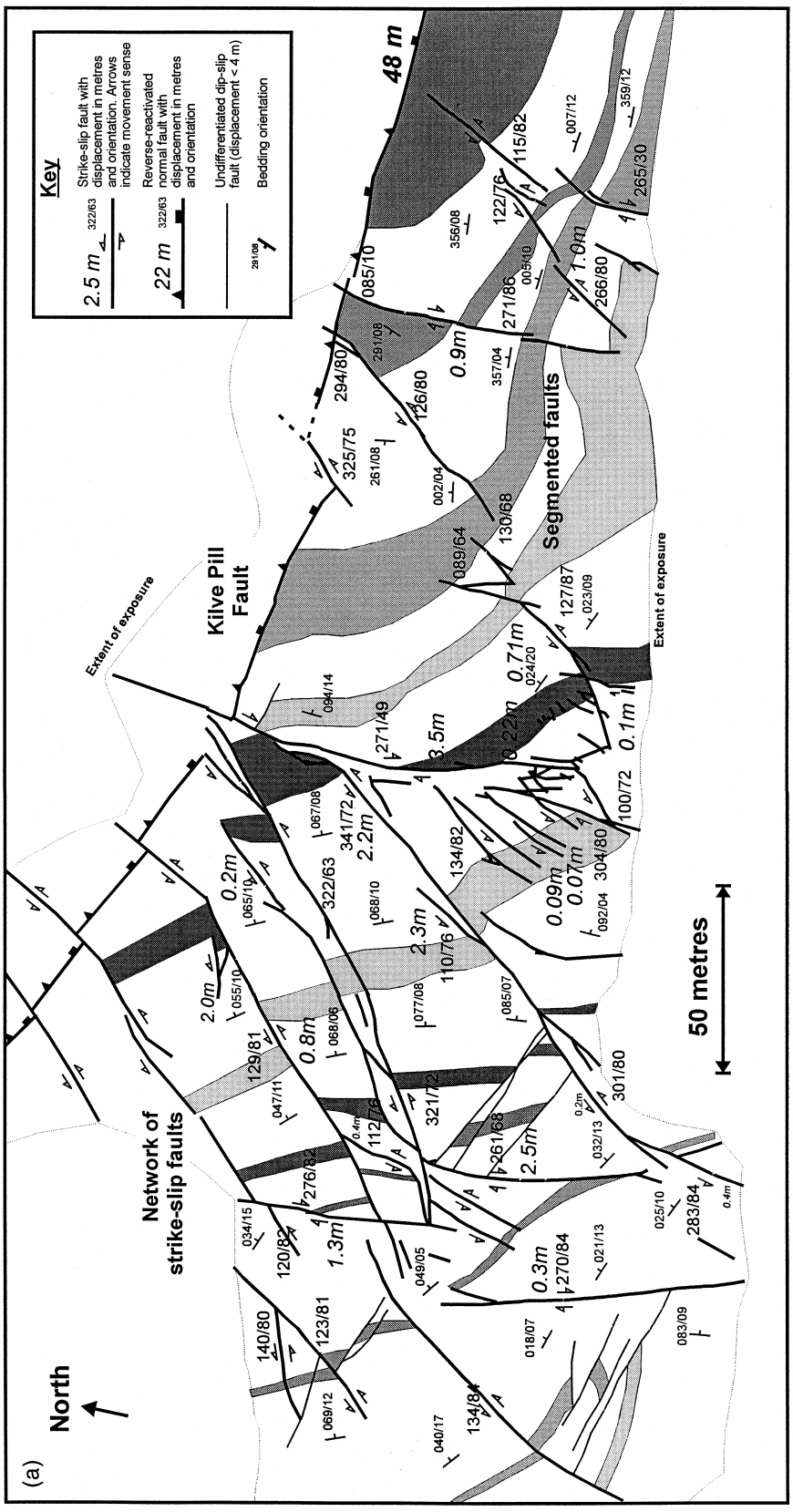

Fig. 3. (a). Map of the strike-slip fault network between the two major reverse-reactivated faults (see Fig. 2 for location). The strike-slip faults form a linked network within the overlapping faults to the west of the map, and are far more segmented on the periphery, to the east. (b) Equal area stereographic projection of dextral and sinistral faults, and slickenside lineations.

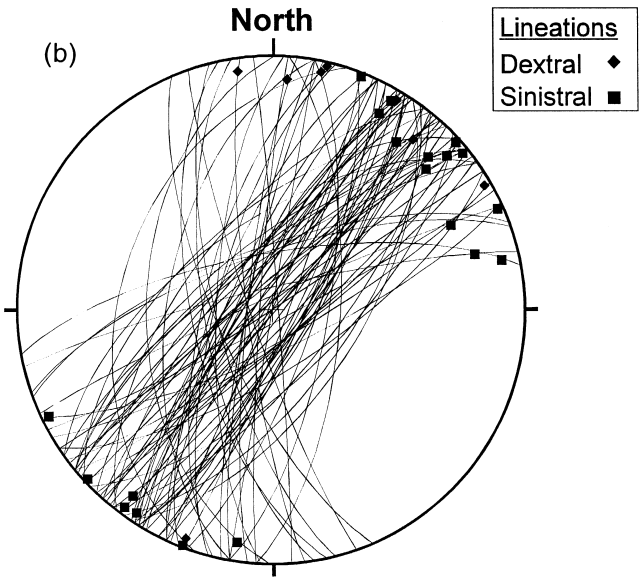

Fig 3 (*continued*)

to sub-horizontal gypsum veins occur with sub-vertical mineral fibres, in the footwall of a reverse-reactivated normal fault. Sibson (1995) suggests the veins are filled with fluids that migrated into a footwall dilational area, created during reverse-reactivation.

3. Selective reverse-reactivation

To investigate the importance of fault geometries on the selective reverse-reactivation of the normal faults (Fig. 2), the properties of normal faults and reverse-reactivated normal faults are compared (Table 1 and Fig. 4). Fault dips and slickenside lineation orientations have similar distributions (Fig. 4a and b). All faults with finite normal displacements >22 m show evidence of reverse-reactivation (Fig. 4c). Reverse-reactivated faults with lesser displacements occur, but it is not possible to calculate the pre-reactivated normal displacements. Note, however, that reverse-reactivation of the 200 m throw Blue Ben Fault (at A, Fig. 2) has not been directly proven, although it does have thrusts in its hanging wall. The maximum observed reverse displacement is 32 m (49° dip) and is within the Blue Ben Fault damage zone (at A, Fig. 2). The faults with the largest finite reverse displacements (up to 32 m) have dips in the range of 40–55°, and the faults with the largest finite normal displacements (23–60 m) have dips $>60°$ (Fig. 4c). Sibson (1995) found an optimum angle between σ_1 and the fault plane for reactivation of normal faults of 25–30°. Further displacement is inhibited at twice this value (i.e. 50–60°) unless pore fluid pressures are sufficient (Sibson, 1985, 1995). The distribution of reverse displacements (Fig. 4c) indicates that the optimum fault dips for reverse-reactivation of the studied faults lie in the range 40–55°, and net reverse movement is rarely achieved on faults with steeper dips. The reverse-reactivated normal faults with dips $<40°$ also have mostly finite extensional displacements <15 m. The net displacements of these faults indicate either (1) optimally oriented faults where normal displacement $\approx$ reverse displacement

Table 1
Comparison of the displacements and dips of the south-dipping and north-dipping normal and reverse/reverse-reactivated normal faults. Faults are included that have dip directions 30° either side of north and south. Negative displacement values refer to reverse displacements, and positive values to normal displacements

			Dips (degrees)			Net displacements (m)		
	Dip direction	No.	Range	Mean	SD	Range	Mean	SD
Normal	North	58	24–86	51.41	14.74	0.1–20.0	3.23	4.66
	South	19	31–80	60.05	12.40	0.1–22.0	7.87	7.09
Reverse	North	23	20–82	44.83	17.35	−32.0–+48.6	4.55	17.11
	South	12	41–72	59.67	8.65	−8.2–+60.0	10.29	19.26

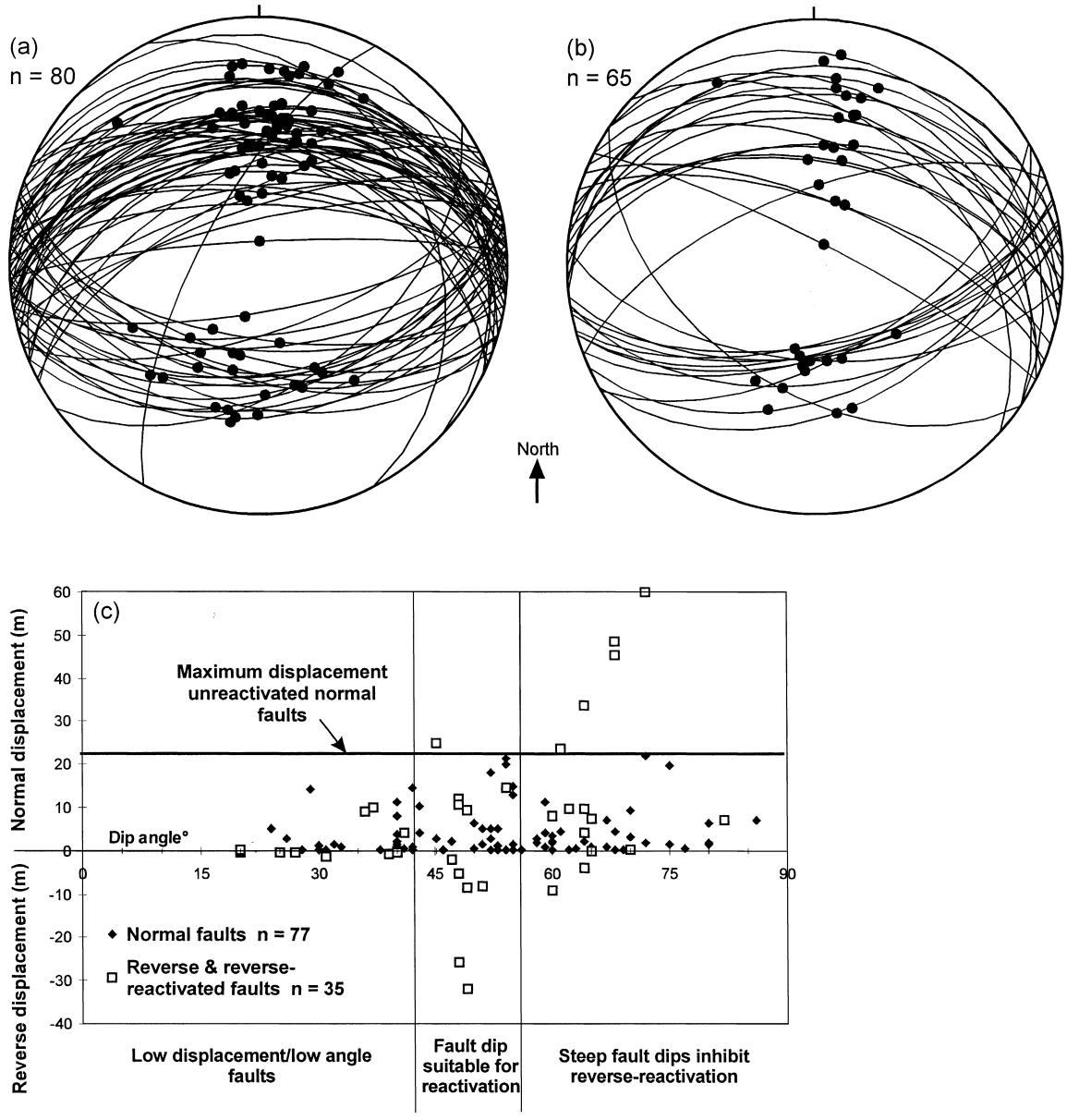

Fig. 4. Comparison of the properties of normal and reverse-reactivated faults. Equal area stereographic projection of fault plane and slickenside lineation orientations for (a) normal faults and (b) reverse and reverse-reactivated normal faults. (c) Graph of displacements plotted against dip angle for normal, reverse and reverse-reactivated faults (negative values indicate reverse displacements). Reverse and reverse-reactivated normal faults are considered together, as it was impossible to distinguish the nature of the faults on the wave-cut platform.

(with faults of any size), or (2) the faults did not have optimal dips for reactivation, and the reverse movement was restricted and relatively minor. Reverse faults with shallow dips (i.e. $\leq 30°$) are likely to have initiated during the contraction event (Fig. 4c), some of which are footwall shortcuts (Huyghe and Mugnier, 1992; Sibson, 1995) or antithetic backthrusts (Hayward and Graham, 1989) to reverse-reactivated normal faults (Fig. 2).

Factors other than fault dip that may influence selective reactivation include fault-plane friction, rotation of domino blocks during basin extension, displacement magnitude and fault connectivity (i.e. a percolation model). The different mechanisms are described below.

3.1. Fault-plane friction

There are differences between the fault geometry and fill that are related to the magnitude of displacement. Faults with low displacements ($<$ bed thickness) have irregular surfaces that are steeper in the limestone units and shallower in the more ductile shales (Fig. 5a). Larger faults with several metres of throw, includ-

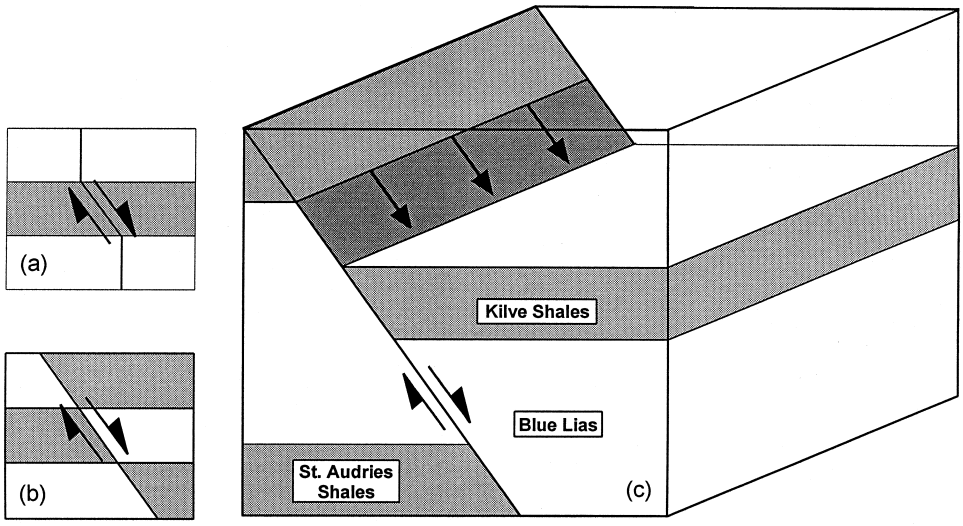

Fig. 5. (a) Schematic diagram to show how steep faults initiate in the more brittle layers (white), but have shallower profiles in the less brittle layers (shaded) (Peacock and Sanderson, 1992; Peacock and Zhang, 1994). (b) The faults assume a shallower, smoother profile during movement of brittle layers past less brittle layers. (c) Block diagram to illustrate how fault gouge can occur along faults that have large enough displacements to juxtapose limestones against the shale-dominated units. Smaller displacement faults wholly within the Blue Lias are less likely to contain gouge material.

ing the Kilve Pill Fault (at B, Fig. 2), have smooth planar surfaces (Fig. 5b). The low displacement normal faults are often healed by calcite fills, but the faults with metre-scale throws are often open with calcite on their surfaces.

The larger normal faults (>25 m) would have displaced the St. Audrie's or Kilve Shales (cf. Fig. 2) and would therefore be most susceptible to shale smear (Fig. 5c). Fault-plane smoothness (Scott et al., 1994; Dragoni and Piombo, 1993), the presence or absence of fault gouge (Marone, 1995; Sibson, 1995), gouge thickness (Koestler and Ehrmann, 1991; Beeler et al., 1996) and composition (Scott et al., 1994) all have an impact on fault-plane friction. Marone (1995) shows experimentally that faults without gouge have higher frictional strengths and fail in a similar way to intact rock. In summary, the field evidence and studies of fault gouge indicate that it is the larger faults that

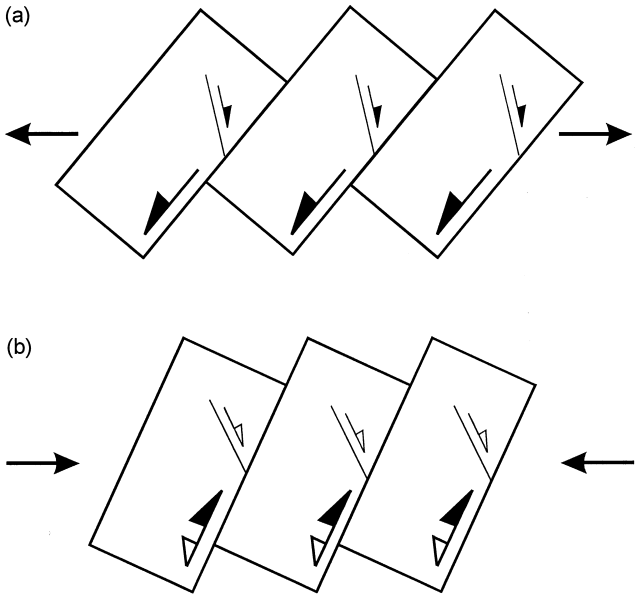

Fig. 6. Rotation of the fault blocks occurs during extension (a), which can be reversed during contraction (b). The master faults undergo the largest rotations to shallower dips, and smaller antithetic faults will be rotated to steeper dips during extension, and therefore make greater angles with σ_1 during the contraction. The filled arrow heads indicate the displacement sense of the active faults in each diagram; the unfilled arrow heads indicate inactive faults. The latest sense of movement is indicated by the filled arrows on the double-headed symbols.

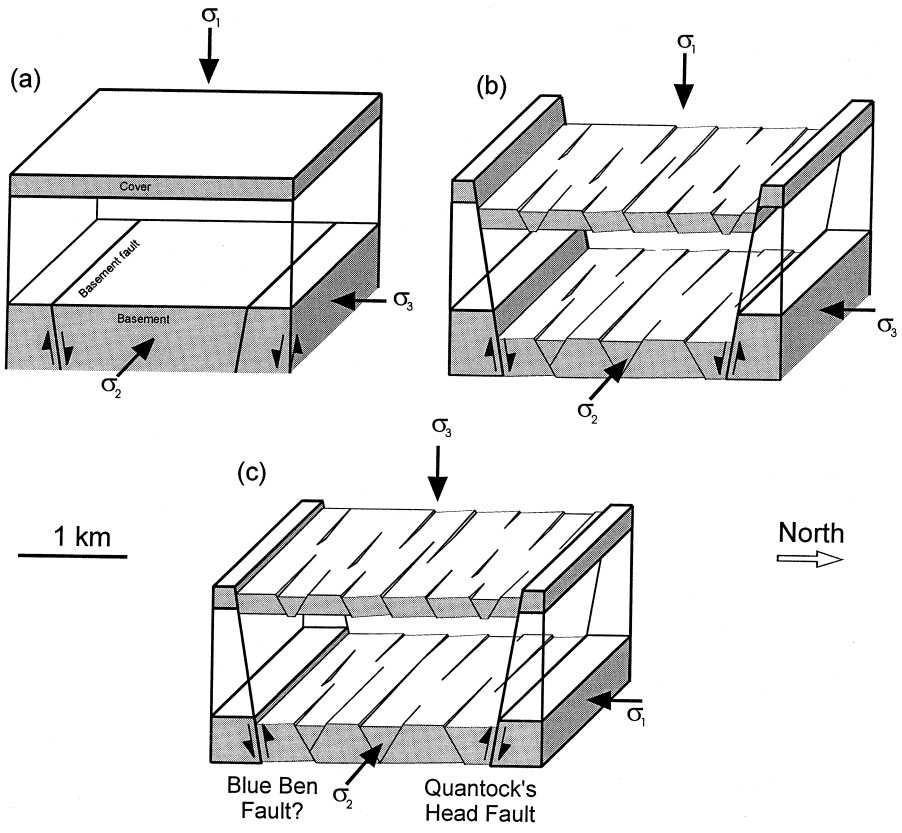

Fig. 7. Model for basement-involved reverse-reactivation in Somerset (modified from a model for the faulting at Flamborough Head, Peacock and Sanderson, 1994b). The orientations of the maximum (σ_1), intermediate (σ_2) and minimum (σ_3) principal compressive stresses are shown. (a) E–W-striking 'basement' faults occur, with the Jurassic being a 'cover' sequence. (b) The basement faults were normally-reactivated after Jurassic deposition and have the largest normal displacements. A network of new normal faults developed throughout the sequence. (c) The basement faults show reverse-reactivation, but the younger faults that do not extend to the basement (represented using finer lines) were not reactivated.

have the lowest frictional strengths due to the likelihood of movement past a shale unit, and have smoother planes that formed from attrition during displacement accumulation. The fault-plane friction model permits the initiation of selective reverse-reactivation of gouge-filled, smooth faults and its subsequent cessation due to gouge thinning and extrusion (Scott et al., 1994).

3.2. Domino block rotation

There is evidence for steepening of the larger south-dipping reverse-reactivated normal faults through reverse-rotation (e.g. the Quantock's Head Fault and the fault that passes through the Blue Ben Headland), as adjacent antithetic faults have considerably shallower dips (Fig. 2). In the areas where neighbouring faults have similar displacements, dips are similar for both north- and south-dipping faults. Faults that dip in the same direction as the beds may have been steepened during regional tilting, but this is not apparent in the gently south-dipping beds in the study area as many south-dipping faults dip at $< 50^\circ$, and there are numerous examples of steep north-dipping faults (Figs. 2 and 4). Normal faults can rotate to have dips of around 25–30° (Sibson, 1995) during domino-style extension (e.g. Gibbs, 1987; Mandal and Chattopadhyay, 1995), with the greatest rotations occurring across the largest displacement faults (Fig. 6a). Faults antithetic to the large displacement faults would be rotated to higher dips which are unfavourable for reactivation (e.g. Sibson, 1985). Faults become locked when the angle between σ_1 and the fault plane exceeds the value determined by doubling the optimum reactivation angle (Sibson, 1995). Reverse-rotation of the faults and hence steepening of their dips would occur during a later contractional stage (Sibson, 1995) (Fig. 6b).

3.3. Fault size

Peacock and Sanderson (1991) show a fault with 0.4 m throw that has a map length of 80 m. A normal fault with 20 m throw would be expected, with the same displacement–length relationship, to be in the order of 4 km in map length, so could cut through the whole of the Jurassic sequence and into the Triassic marls below. A similar model to that for the faulting

at Flamborough Head, East Yorkshire, may be appropriate, where the reactivation may have been driven by stresses in the basement (Peacock and Sanderson, 1994b; Peacock, 1996) (Fig. 7). At Flamborough Head, E–W-striking basement faults that developed during the Jurassic (Kirby and Swallow, 1987), and may extend back to the Carboniferous (Rawson and Wright, 1992), were reverse-reactivated (Peacock and Sanderson, 1994b; Peacock, 1996). Normal faults in the cover, initiated in the Cretaceous, have a wide range of orientations, and were not reverse-reactivated (Peacock, 1996). Faults in the Jurassic 'cover' in Somerset may have become detached from the Triassic 'basement', above one of the anhydrite units in the Mercia Mudstone (Warrington and Scrivener, 1980; House, 1993), and were not reactivated. The faults which extend from the Triassic 'basement' to the Jurassic 'cover' are more likely to be reactivated than the faults that are small enough to be contained entirely within the 'cover' if the reactivation was driven by stresses in the basement. A detachment model was proposed by Roberts et al. (1990) to illustrate the reverse-reactivation of faults in the Central Graben of the North Sea. In their model, an antithetic backthrust propagated from the reverse-reactivated fault, along a salt horizon which detached the Jurassic–Cretaceous sequence from the basement. The Jurassic–Cretaceous sequence was then shortened independently by folds above the tip of the backthrust (Roberts et al., 1990).

Sibson (1995) proposed that a population of gypsum veins in the footwall of a reverse-reactivated normal fault within the Triassic marls exposed at Watchet (Fig. 1) indicates over-pressured fluid expulsion during fault-valve activity. Fluids accumulate in hydrofractures within impermeable strata adjacent to unsuitably oriented faults, and are expelled into the fault when the fluid pressure exceeds σ_1 and σ_3 (Sibson, 1995). A mechanism is thereby provided by which the reactivation could have affected only those normal faults large enough to continue beyond the limestones into the less permeable units, such as the deeper Triassic marls.

3.4. Percolating network of connected faults

A cross-section of the Quantock's Head area (Fig. 8, line is shown in Fig. 2) illustrates the spatial distribution of the reverse-reactivated faults. Projection above the present-day beach level of the Quantock's Head Fault and the 25 m displacement fault to the north, indicates that an intersection between the two would have occurred. These two faults are the only two reverse-reactivated faults on the section. The unreactivated faults have displacements of <1 m, and appear isolated. One exception is an unreactivated fault inside the conjugate intersection of the reverse-reactivated faults, which links to the north-dipping fault.

The importance of fault connectivity in the selective

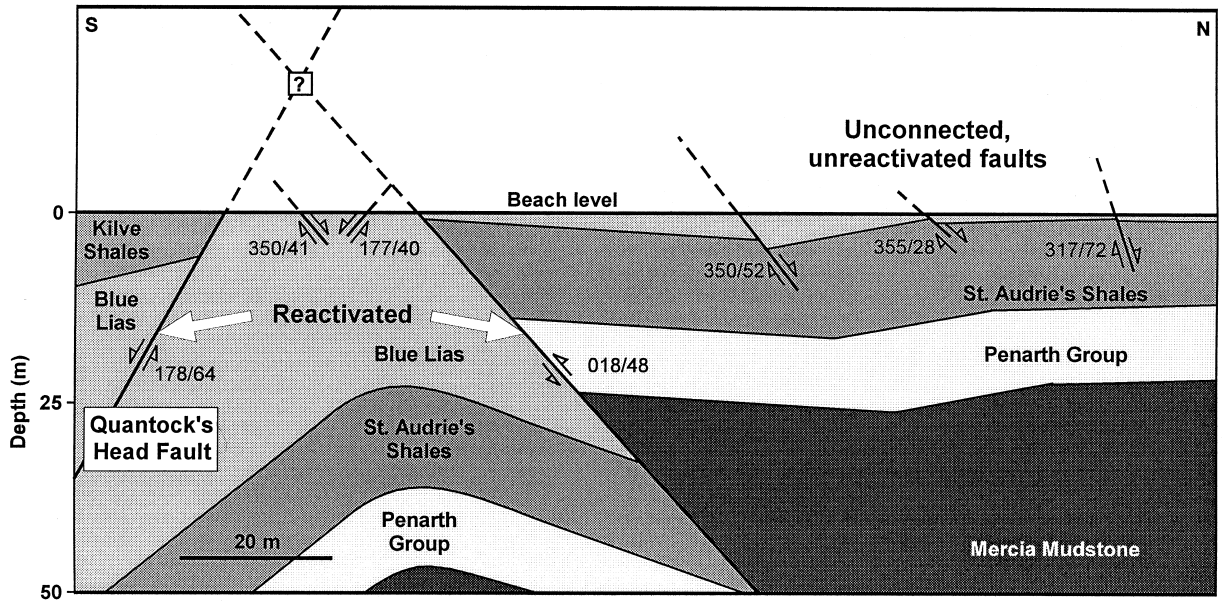

Fig. 8. Cross-section of the Quantock's Head region (see Fig. 2 for the cross-section location). Fault dimensions were determined from the juxtaposed units and fault displacements. In the absence of three-dimensional control on fault geometries, maximum displacements were assumed at the surface, and a standard displacement–length (D–L) relationship of $D \propto L^2$ was applied (i.e. radial fault planes, Walsh and Watterson, 1988). All the faults have equal lengths above and below the surface, based on the assumption that displacement maxima occur at a fault's centre (Barnett et al., 1987). Deformation is concentrated on a network of large displacement, connected faults that extend through the sequence. The smaller, poorly-connected faults are not reactivated.

reverse-reactivation of the normal faults can be demonstrated with a percolation model (e.g. Stark and Stark, 1991; Turcotte, 1995; Sahimi and Arbabi, 1996). A single percolation network on the Somerset coast would involve linkage of the reverse-reactivated Quantock's Head and Kilve Pill Faults (C and B, Fig. 2) which have opposing dips and are separated by a horst. Linkage of both the Quantock's Head and Kilve Pill Faults to an underlying fault (the Central Bristol Channel Fault Zone, Brooks et al., 1988) would form a network of larger faults upon which the reverse-reactivation was concentrated. The passage of fluids through the basin would preferentially occur along the connected network of normal faults that form the backbone of the percolation cluster (e.g. Quantock's Head Fault, Fig. 8). Isolated, poorly connected or impermeable faults are not reactivated. Connectivity in itself does not guarantee that a fault will form part of the percolation backbone, as fluid flow through a network relies on fault permeability (Stauffer and Aharony, 1992). Fluid discharge during fault-valve action is typical of steep faults (Sibson, 1995), but fluid migration through the basin, and consequently reverse-reactivation, would focus along faults of any orientation, with sufficient permeabilities that are connected to the source.

4. Geometries of overlapping and underlapping zones

In normal fault systems, displacement at an overlap zone in map view is transferred from one synthetic fault segment to another across a relay ramp (e.g. Larsen, 1988; Peacock and Sanderson, 1991, 1994a; Trudgill and Cartwright, 1994), or via an accommodation zone between two opposite polarity faults (Morley et al., 1990; Gawthorpe and Hurst, 1993; McClay and White, 1995). Underlap zones occur between two offset synthetic fault segments, whose tips have not propagated past each other (Peacock and Sanderson, 1991). In contractual systems, a transfer zone is defined as the zone between two overlapping thrust planes that link at depth to a décollement (Dahlstrom, 1969; Boyer and Elliott, 1982). In map view, approximately uniform contraction is conserved across the transfer zone by the cumulative shortening of en échelon, sub-parallel faults and folds in the hanging walls of thrusts (House and Gray, 1982), with displacement along the thrusts decreasing into the transfer zone. Alternatively, Lebel and Mountjoy (1995) use numerical modelling to show that displacement minima and maxima along a thrust, in map view, can occur through systematic shifting of the deformation from one thrust to another. Displacement

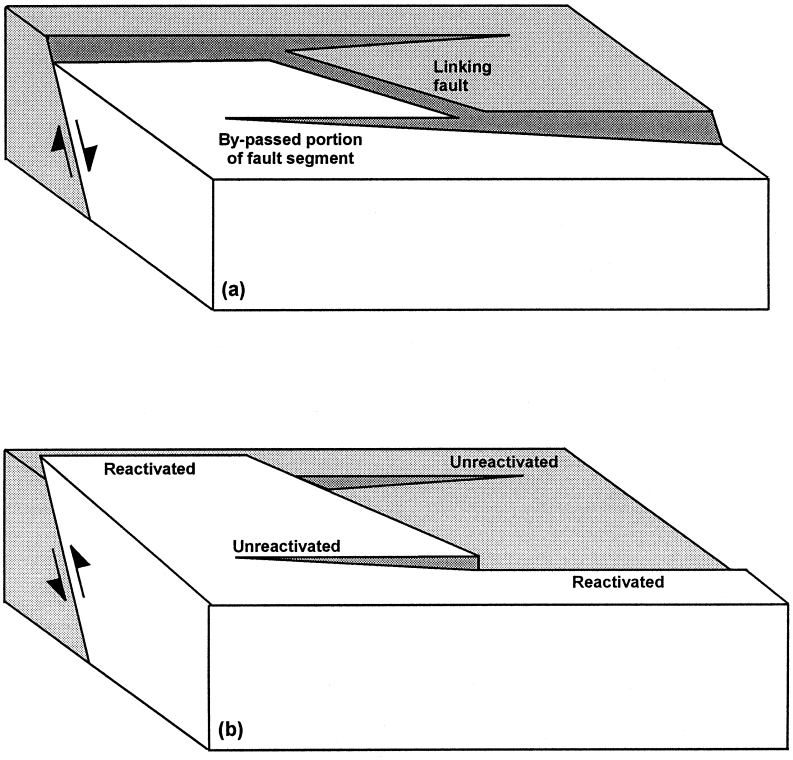

Fig. 9. (a) Schematic drawing of a relay ramp in a reverse-reactivated normal fault system. (b) Model to illustrate the style of faults at transfer zones between reverse-reactivated fault segments.

on the most suitably oriented and positioned thrust occurs until movement is prevented, and the shortening is accommodated by another thrust (Lebel and Mountjoy, 1995).

In reverse-reactivated normal fault systems, the style of displacement accommodation is governed by the geometry of the pre-existing normal fault network, and by the selective reactivation of some of those normal faults. For example, relics of normal fault relay ramps (Larsen, 1988; Peacock and Sanderson, 1991, 1994a; Trudgill and Cartwright, 1994) that formed during the extension event (Fig. 9a) are often preserved adjacent to the reverse-reactivated normal fault. The throughgoing fault is reverse-reactivated, but the fault tips bypassed during breaching of the relay ramp are not reactivated (Fig. 9b). Several examples of breached relay ramps, between fault segments with spacings <1 m, occur within the reverse-reactivated Kilve Pill Fault Zone (at B, Fig. 2).

Shortening between antithetic reverse-reactivated normal faults has been accommodated by (1) a strike-slip fault network within an overlap zone (at D, Figs. 2 and 3a), and (2) an array of obliquely oriented reverse faults at an underlap zone (at E, Fig. 2). Both of these occur between two steep ($\geq 60^{\circ}$) reverse-reactivated normal faults (Fig. 2). The traditional definition of a thrust transfer zone (Dahlstrom, 1969; Boyer and Elliott, 1982) does not apply to these examples, as they occur between faults with opposing dips, rather than between faults with similar dip directions that link at

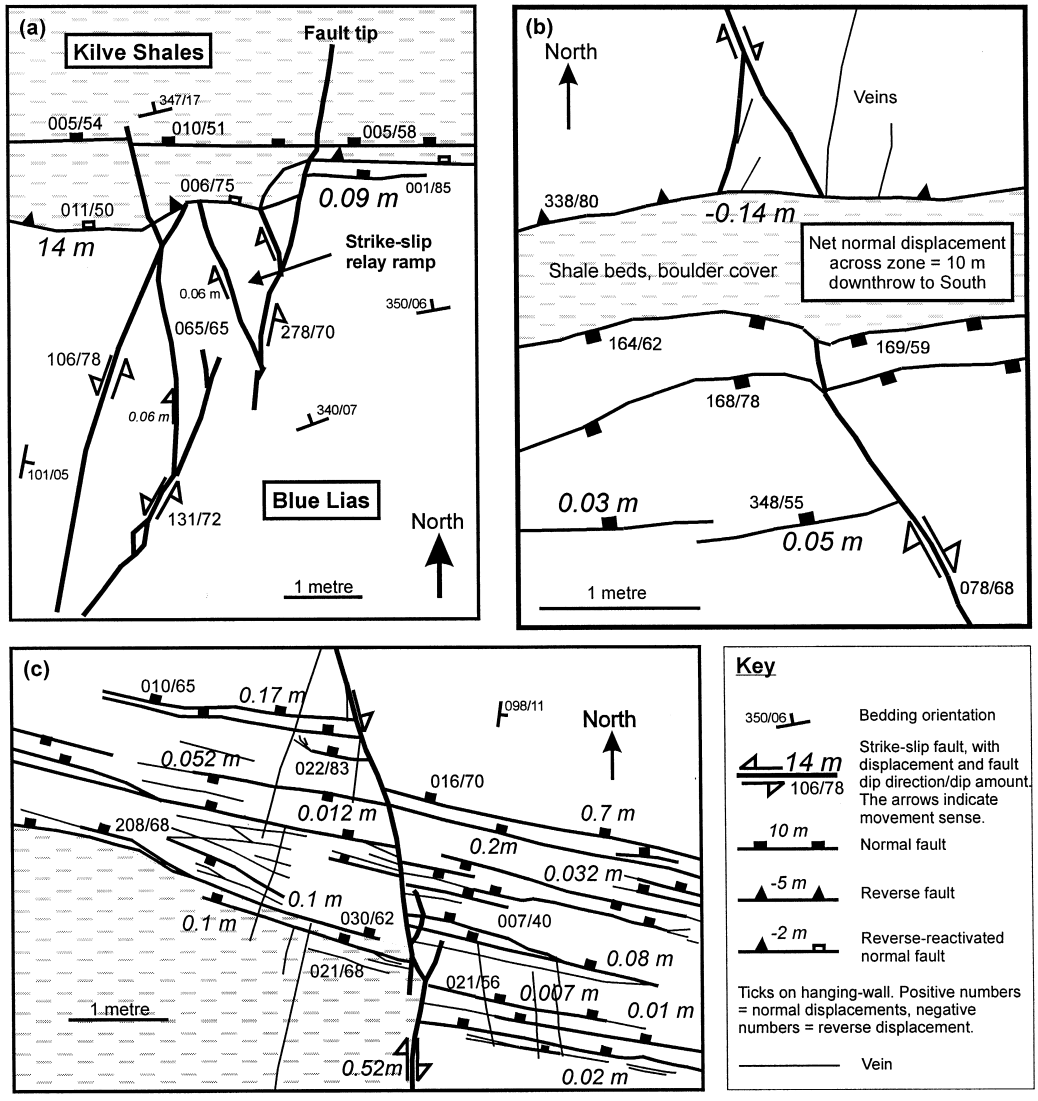

Fig. 10. Maps of strike-slip faults at intersections with earlier E–W-striking dip-slip faults on the Somerset coast; the shading represents shale beds, and the limestone beds are unshaded. (a) Intersection of a sinistral strike-slip fault zone that includes a relay ramp, and a reactivated normal fault zone. The antithetic right-lateral faults within the relay ramp are truncated at the normal fault and the main segment has propagated through, but ends shortly after intersection in the Kilve Shales. (b) Right-lateral strike-slip faults terminate at reverse faults, and bend into the normal faults. (c) The right-lateral strike-slip faults cross-cut an unreactivated normal fault zone.

depth. The style of shortening accommodation is dependent on the structural heterogeneity inherited from the extensional phase of basin development, i.e. fault spacing and whether the faults overlap or underlap. For example, the strike-slip network (Fig. 3a) is between two reverse-reactivated normal faults that define a zone 500 m wide that contains relatively few normal faults.

4.1. Strike-slip network

A network of conjugate strike-slip faults occurs within a horst block, at an overlap between the south-dipping Quantock's Head Fault and the north-dipping Kilve Pill Fault (at D, Figs. 2 and 3a). The amount of overlap between the two reverse-reactivated normal fault zones is not known, as the tips of both faults are not exposed. The zone containing the strike-slip fault network is wholly within the interbedded Blue Lias limestones and shales. The Blue Lias is between the more ductile Kilve Shales and St. Audrie's Shales, and strike-slip faults in the shale units to the north of the Kilve Pill Fault are rare (Fig. 2). There is a marked change eastwards from a linked network of conjugate strike-slip faults in the overlap zone with displacements of a few metres, towards a highly segmented strike-slip fault system with displacements of < 1 m (Fig. 3a).

4.2. Interaction of strike-slip and dip-slip faults

There have been conflicting views on the relative timing of the strike-slip fault development and reverse-reactivation of the normal faults. To generate strike-slip faulting and reverse-reactivation of normal faults during one event, σ_3 and σ_2 must have been able to swap, at least locally. Dart et al. (1995) state that the strike-slip faults formed after the reverse-reactivation of the normal faults, but Nemcok et al. (1995) believe that the two modes of faulting were contemporaneous. A relative chronology is evident, however, from maps of cross-cutting strike-slip and dip-slip faults (Fig. 10).

Three distinct styles of fault intersections occur where rare examples of strike-slip faults cross-cut normal and reverse-reactivated normal faults (Fig. 10). (1) The main left-lateral fault crosses beyond the intersection point but terminates within a few metres of the dip-slip fault (Fig. 10a). Minor right-lateral faults abut both the main left-lateral fault and the reverse-reactivated normal fault. (2) All strike-slip faults terminate at reverse-reactivated normal faults (Fig. 10b). (3) The strike-slip faults displace the normal faults without any interaction (Fig. 10c).

An apparent termination of a strike-slip fault against a reverse-reactivated normal fault may be the result of movement of the latter after the strike-slip fault event (Fig. 10a and b). However, antithetic faults form after the establishment of a strike-slip relay ramp between a pair of master faults (Peacock and Sanderson, 1995), so the truncated antithetic strike-slip faults initiated after one of the faults that now offsets the reverse-reactivated normal fault (Fig. 10a). Using joint interaction studies (Dyer, 1988) as an analogy, the termination of one fault at another is attributed to the propagating tip of the strike-slip fault encountering the free surface of an open fault. A free surface exists along a reverse-reactivated normal fault that is jacked open by overpressured pore fluids (Sibson, 1995), or during movement. The examples shown in Fig. 10(a) and (b) indicate that during strike-slip fault development the E–W faults were able to be reactivated, but in Fig. 10(c) the normal faults were healed and not reactivated. These examples (Fig. 10) therefore indicate that the strike-slip faults developed either during or prior to the reversal of the normal faults, but not after (cf. Dart et al., 1995).

The role of strike-slip faults in basin inversion has been reported by Chadwick (1993) and Cloke et al. (1997), who recognised transfer faults between reverse-reactivated normal faults. However, the strike-slip faults in Fig. 3(a) are not transfer faults (e.g. Davison, 1994), but have instead accommodated shortening of the overlap zone between the two reverse-reactivated normal faults. The intensity of strike-slip deformation decreases outwards from the centre of the overlap (i.e. from a linked network to isolated strike-slip faults).

Three sets of strike-slip faults in the overlap have been identified (Figs. 2 and 3a), and a relative chronology has been established which is similar to that for strike-slip relay ramps (Peacock and Sanderson, 1995):

1. A set of three sub-parallel NE-trending sinistral faults with a c. 90 m spacing, between the Quantock's Head Fault and the Kilve Pill Fault that divide the overlap into blocks (*block-bounding faults*) (at F, G and H, Fig. 2). Block rotation between the strike-slip faults is evident from the clockwise rotation of the Kilve Pill Fault.
2. Dextral strike-slip faults with NNW strikes often offset the block-bounding sinistral faults, indicating that they are more recent.
3. Sinistral faults between the block-bounding faults have more easterly strikes, and are generally shorter and often offset the dextral faults.

The last two sets are collectively termed *intra-block faults* in the following sections.

Antithetic faults that delimit rotating blocks commonly occur in overlaps between sub-parallel, synthetic strike-slip faults, e.g. on the km-scale between the San Andreas and San Jacinto Faults (Nicholson et al., 1986), and on the mm-scale to the west of the Blue Ben Headland (at A, Fig. 2) (Kelly, 1996). The lo-

cation of the sinistral block-bounding faults therefore suggests a component of dextral movement along one, or both, of the reverse-reactivated normal faults, prior to development of the intra-block faults. Block-bounding faults with sinistral displacements and sub-horizontal slickenside lineations could not have formed if either the Quantock's Head or Kilve Pill Faults had a sinistral component in this locality.

Immediately west of the western block-bounding fault (F, Fig. 2) there are two reverse faults that strike northwest and are therefore oblique to the Quantock's Head Fault, but sub-parallel to the rotated Kilve Pill Fault. These faults strike obliquely to the majority of the normal faults on the foreshore, which they displace. The single set of slickenside lineations on the obliquely-oriented faults indicate reverse dip-slip movement, and therefore new thrusts that formed during the contraction. The strike of these two reverse faults and the acute dihedral angle bisector for the intra-block faults indicate that these faults formed with a local NE-trending σ_1 orientation. The formation of the sinistral block-bounding faults, and the development of new oblique reverse faults can be combined into a dextral transpression model (Sanderson and Marchini, 1984); dextral movement is indicated by the block rotations, and contraction by reverse-reactivation (Fig. 11). In this model, the sinistral block-bounding faults form, and rotate the Kilve Pill Fault. The shortening direction within the overlap is modified by the new orientation of the Kilve Pill Fault, and the curved trace of the Quantock's Head Fault. Contraction of the overlap then dominates, and is accommodated by the formation of the conjugate intra-block faults, and reverse faults at the base of the western rotating block

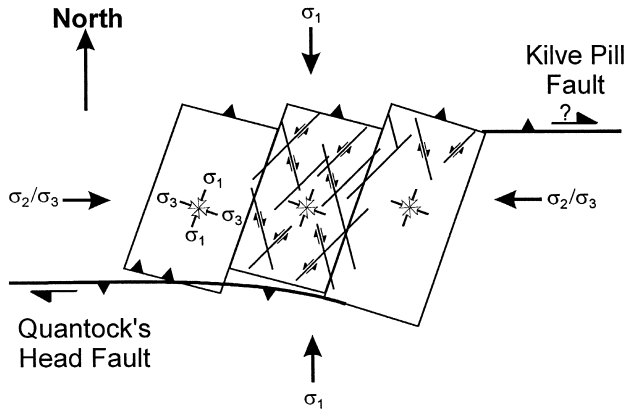

Fig. 11. Schematic diagram to illustrate a mechanism for the formation of the strike-slip network in the overlap between the Quantock's Head and Kilve Pill Faults. Dextral transpression (Sanderson and Marchini, 1984) causes the formation of sinistral faults and block rotation. The shortening is accommodated by the formation of thrusts at the southern end of the block, that are oblique to the Quantock's Head Fault. Unfilled arrows = local stress axes, filled arrows = 'regional' stress axes.

(Figs. 2 and 11). The transfer of movement between the reverse-reactivated normal faults, reverse faults and the strike-slip network is an example of systematic shifting from one structural style to another to accommodate the contraction through time (cf. Lebel and Mountjoy, 1995).

4.3. Oblique, steeply-dipping reverse faults

In an underlap region between the western tip of the Quantock's Head Fault and a north-dipping reverse-reactivated normal fault to the northeast of the Blue Ben Headland (at E, Fig. 2), there is an array of NE-striking reverse faults with $>40^\circ$ dips which occur on the rim of a syncline. The beds dip gently towards the southeast in the hanging walls of the reverse faults, and are sub-horizontal in the footwalls (Fig. 2). The fault dips suggest that they originated as normal faults, but their strikes are inconsistent with N–S extension. If the faults formed during the extensional phase of basin development, and were reverse-reactivated during N–S shortening, there might be evidence of oblique-slip. The slickenside lineations however indicate that these faults are predominantly dip-slip, and are therefore probably reverse faults that developed during the contraction.

Possible methods by which NE-striking reverse faults could have developed at this locality include: (1) a previously unrecognised phase of northwest shortening, (2) sinistral transpression (Sanderson and Marchini, 1984), and (3) loading of the corner of the underlap zone. Regional northwest directed shortening is rejected through lack of evidence, but the stress system could have been modified locally by other fault movements to form these structures.

Slickenside lineation orientations at the western end of the Quantock's Head Fault (Fig. 2b) are consistent with a component of sinistral strike-slip movement, although dip-slip dominates. The slickenside lineations on the northern fault indicate almost pure dip-slip movement, so sinistral movement of the Quantock's Head Fault would have been the dominant factor in a transpression model. The sinistral transpression model does not, however, account for the steepness of the reverse faults.

A third possibility is that the reverse faults formed during loading of the corner of the underlap zone by the hanging wall of the Quantock's Head Fault (Fig. 2). In this model, an anticline with a NE–SW-trending axis initially formed with a steeper southeast limb, due to the applied load (Fig. 12). The beds in the south of the fold hinge dip towards the loaded corner of the underlap zone to the ESE, whilst those in the footwall dip WNW. Further shortening of the underlap, driven by sustained movement of the hanging wall of the Quantock's Head Fault, caused the anticline to fail

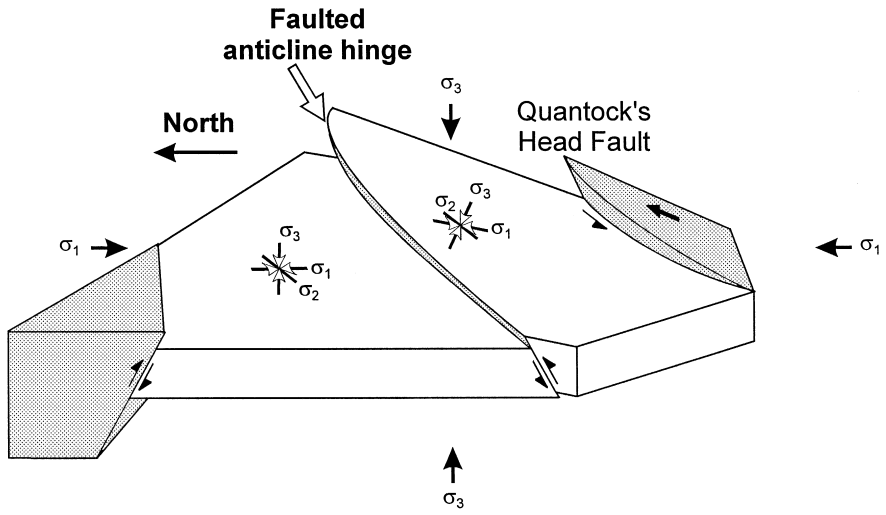

Fig. 12. Block diagram to illustrate the interpretation of the formation of obliquely-oriented high-angle reverse faults east of the Blue Ben Headland. A NE–SW-trending anticline forms initially, due to loading of the corner of the underlap zone by the hanging wall of the Quantock's Head Fault. The beds in the south of the fold hinge dip towards the loaded corner of the underlap zone to the ESE, whilst those in the footwall dip WNW. Continued shortening, driven by the northwards movement of the Quantock's Head Fault hanging wall, causes failure along the anticline hinge, and new NE-striking reverse faults develop. Open arrows = local stress axes, closed arrows = 'regional' stress axes.

along the hinge, by means of NE–SW-striking reverse faults.

5. Deformation model

The geometries of the under- and overlap zones provide evidence to support a single progressive deformation event, during which the method by which shortening was accommodated switched between reverse-reactivation of normal faults, reverse faults and conjugate strike-slip faults. The sinistral movement identified at the western end of the Quantock's Head Fault (Fig. 2b), the dip-slip displacement at the centre and the postulated dextral motion at its eastern end (Fig. 11) imply that the footwall of the Quantock's

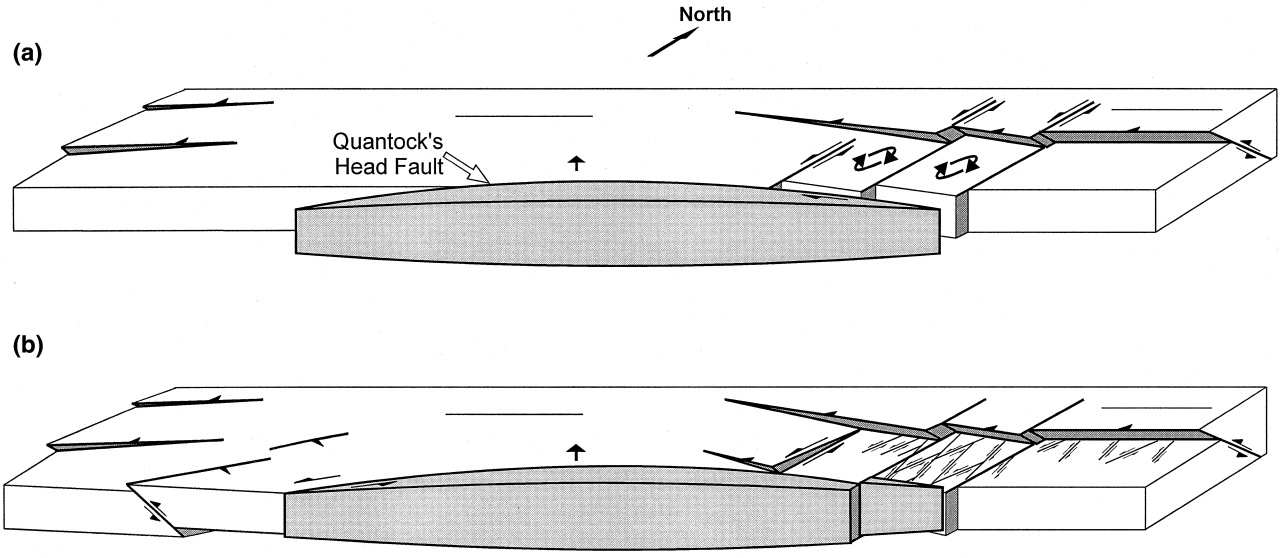

Fig. 13. Block diagrams to illustrate the incorporation of the contractional deformation in the Quantock's Head area into a single on-going event, controlled by the reverse-reactivation of the Quantock's Head Fault. (a) The Kilve Pill Fault is displaced and rotated clockwise by sinistral faults that form in response to dextral transpression along the Quantock's Head Fault. The local principal stress axes and existing structures are rotated anti-clockwise to the west, and clockwise to the east, of the Quantock's Head Fault during its northwards movement. (b) Sustained horizontal, northwards movement of the Quantock's Head Fault causes σ_1 to be perturbed such that reverse faults oblique to existing faults form in an underlap to the west of the Quantock's Head Fault. To the east of the Quantock's Head Fault, a network of conjugate strike-slip faults develops, that suggests a NNE σ_1 orientation.

Head Fault was deformed around its hanging wall in map view. In addition, approximately N–S contraction of the hanging wall is evident from thrusts (Peacock and Sanderson, 1992) and a hanging wall buttress anticline (Dart et al., 1995).

It is commonly accepted that the contraction-related structures in the Wessex and Bristol Channel Basins are an expression of Alpine tectonism (Van Hoorn, 1987; Brooks et al., 1988; Chadwick, 1993; Dart et al., 1995; Nemcok et al., 1995), i.e. approximately N–S oriented shortening, and in the preceding sections the role of the Quantock's Head Fault has been analysed and discussed. For example, the obliquely-oriented reverse faults are unique to the underlap zone close to the termination of this fault (at E, Fig. 2), and suggest that movement of the Quantock's Head Fault was instrumental in their formation (Fig. 12). The dip-slip faults to the northeast of the curved trace of the Quantock's Head Fault strike ESE, while those to the northwest strike ENE (Fig. 2). The faults could have rotated to their present-day strikes during the contraction, if it is assumed that the orientations of the normal faults were originally similar (i.e. approximately E–W). In models of thrust-belt formation, Marshak et al. (1992) observed pure dip-slip movement at the front of a curved indentor, a dextral component at one end, and sinistral movement at the other extreme. The amount of reverse movement across the Quantock's Head Fault is not quantifiable from the field observations, but the structures analysed in the previous sections indicate that horizontal shortening of its footwall was related to northwards movement of the hanging wall, that may account for its curved trace (e.g. Marshak et al., 1992).

Fig. 13 illustrates how the reverse-reactivation of normal faults, strike-slip fault development and the development of steep and oblique reverse faults can be incorporated into a single deformation model. Deformation is accommodated by:

1. Selective reverse-reactivation of the largest-displacement faults, e.g. the Quantock's Head Fault (Fig. 2), and other normal faults that strike perpendicular to the local σ_1 orientation.
2. (a) Sinistral strike-slip faulting with clockwise block rotation during the reverse movement across the Quantock's Head Fault (Fig. 11). Shortening of the newly-formed blocks accommodated by the strike-slip fault network, that suggests a NNE σ_1 orientation (Figs. 3 and 11), and thrusts at the foot of the blocks. The strike-slip faults have the greatest displacements, and link to form a through-going network in the central block, and are more isolated with smaller displacements outside of the overlap to the east. The offset of the Quantock's Head Fault by one of the sinistral block-bounding faults (F, Fig. 2) accounts for the more intense strike-slip deformation within the central block, i.e. the hanging wall is pushed further north at this point than in the western block. (b) σ_1 is locally perturbed such that reverse faults oblique to existing faults form to the west of the fault, at an underlap with other reverse-reactivated normal faults (Fig. 12).

6. Conclusions

1. Mapped examples of normal faults and reverse-reactivated normal faults suggest that all normal faults with >22 m displacement were reactivated during basin contraction. Some faults with smaller displacements were also reverse-reactivated, and new thrusts propagated, some with displacements of >1m. Reverse-reactivation of the normal faults in Somerset appears to be independent of fault dip.
2. The field observations summarised in Fig. 4(c) suggest that both fault dip and size play major roles in selective reactivation. Possible reasons for the preferential reverse-reactivation of larger normal faults include:

    2.1. Decreased fault-plane friction due to smooth fault profiles and thicker gouges.
    2.2. Domino-style reverse-rotation.
    2.3. Contraction may have been driven from the basement, affecting only the basement-involved larger faults. Smaller faults within the cover sequence remained unreactivated.
    2.4. Deformation and fluid flow was concentrated onto a connected network of larger faults.

3. Fault geometries at overlapping and underlapping zones are controlled by the selective reactivation of normal faults, and in particular the width of the zone. Two styles are recognised: (a) A strike-slip network formed in response to a dextral component on the Quantock's Head Fault, and (b) obliquely-oriented reverse faults that developed during loading of the corner of the underlap zone.
4. Interaction between strike-slip faults and earlier E–W-striking normal faults on the Somerset coast is confined, generally, to reverse-reactivated normal fault zones.
5. All of the contractional structures can be incorporated into a unifying deformation model in which the upward movement of the hanging wall of the Quantock's Head Fault was accompanied by northwards horizontal movement.

Acknowledgements

This work was funded partly by Elf Aquitaine, and

we are grateful for the help of Keith Rawnsley, and his permission to publish. PGK is funded by the University of Southampton, and ACM is funded by NERC. Joe Cartwright and Paul Gillespie reviewed the manuscript, and their contributions are gratefully acknowledged. DCPP thanks R. Sibson for enlightening field discussions.

References

Badley, M.E., Price, J.D., Backshall, L.C., 1989. Inversion, reactivated faults and related structures: seismic examples from the southern North Sea. In: Cooper, M.A., Williams, G.D. (Eds.), Inversion Tectonics (special issue). Geological Society of London Special Publication 44, 201–222.

Barnett, J.A.M., Mortimer, J., Rippon, J.H., Walsh, J.J., Watterson, J., 1987. Displacement geometry in the volume containing a single normal fault. American Association of Petroleum Geologists Bulletin 71, 925–937.

Beeler, N.M., Tullis, T.E., Blanpied, M.L., Weeks, J.D., 1996. Frictional behaviour of large-displacement experimental faults. Journal of Geophysical Research 101, 8697–8715.

Bowyer, M.O.N., Kelly, P.G., 1995. Strain and scaling relationships of faults and veins at Kilve, Somerset, UK. Proceedings of the Ussher Society 8, 411–415.

Boyer, S.E., Elliott, D., 1982. Thrust systems. American Association of Petroleum Geologists Bulletin 66, 1196–1230.

Brewer, J.A., Smythe, D.K., 1984. MOIST and the continuity of crustal reflectors along the Caledonian–Appalachian orogen. Journal of the Geological Society of London 141, 104–120.

Brooks, M., Traynor, P.M., Trimble, T.J., 1988. Mesozoic reactivation of Variscan thrusting in the Bristol Channel area, UK. Journal of the Geological Society of London 145, 439–444.

Chadwick, R.A., 1993. Aspects of basin inversion in southern Britain. Journal of the Geological Society of London 150, 311–322.

Cloke, I.R., Moss, S.J., Craig, J., 1997. The influence of basement reactivation on the extensional and inversional history of the Kutai Basin, East Kalmantan, SE Asia. Journal of the Geological Society of London 154, 157–162.

Cooper, M.A., Williams, G.D. (Eds.), 1989. Inversion tectonics (special issue). Geological Society of London Special Publication 44.

Dahlstrom, C.D.A., 1969. Balanced cross-sections. Canadian Journal of Earth Sciences 6, 743–757.

Dart, C.J., McClay, K., Hollings, P.N., 1995. 3D analysis of inverted extensional fault systems, southern Bristol Channel basin, UK. In: Buchanan, J.G., Buchanan, P.G. (Eds.), Basin Inversion (special issue). Geological Society of London Special Publication 88, 393–413.

Davison, I., 1994. Linked fault systems; extensional, strike-slip and contractional. In: Hancock, P.L. (Ed.), Continental Deformation, pp. 121–142.

Dragoni, M., Piombo, A., 1993. Propagation of an aseismic dislocation through asperities with smooth borders. Physics of the Earth and Planetary Interiors 80, 1–11.

Dyer, R., 1988. Using joint interactions to estimate palaeostress magnitudes. Journal of Structural Geology 10, 685–699.

Enfield, M., Coward, M., 1987. The structure of the West Orkney Basin, northern Scotland. Journal of the Geological Society of London 144, 871–884.

Gawthorpe, R.L., Hurst, J.M., 1993. Transfer zones in extensional basins: their structural style and influence on drainage development and stratigraphy. Journal of the Geological Society of London 150, 1137–1152.

Gibbs, A., 1987. Development of extension and mixed-mode sedimentary basins. In: Coward, M.P., Dewey, J.F., Hancock, P.L. (Eds.), Continental Extensional Tectonics (special issue). Geological Society of London Special Publication 28, 19–34.

Hayward, A.B., Graham, R.H., 1989. Some geometrical characteristics of inversion. In: Cooper, M.A., Williams, G.D. (Eds.), Inversion Tectonics (special issue). Geological Society of London Special Publication 55, 17–39.

House, M.R., 1993. Geology of the Dorset Coast, 2nd ed. The Holywell Press, Oxford Geologists' Association Guide No. 22.

House, W.M., Gray, D.R., 1982. Displacement transfer at thrust terminations in Southern Appalachians—Saltville Thrust as example. American Association of Petroleum Geologists Bulletin 66, 830–842.

Huyghe, P., Mugnier, J.-L., 1992. Short-cut geometry during structural inversions: competition between faulting and reactivation. Bulletin de la Société Geologique de France 163, 691–700.

Kelly, P.G., 1996. Strike-slip faulting and block rotations at Kilve, Somerset. Geoscientist 6, 14–16.

Kirby, G.A., Swallow, P.W., 1987. Tectonism and sedimentation in the Flamborough Head region of north-east England. Proceedings of the Yorkshire Geological Society 46, 301–309.

Koestler, A.G., Ehrmann, W.U., 1991. Description of brittle extensional features in chalk on the crest of a salt ridge (NW Germany). In: Roberts, A.M., Yielding, G., Freeman, B. (Eds.), The Geometry of Normal Faults (special issue). Geological Society of London Special Publication 56, 113–123.

Lake, S.D., Karner, G.D., 1987. The structure and evolution of the Wessex Basin, southern England: an examples of inversion tectonics. Tectonophysics 137, 347–378.

Larsen, P.-H., 1988. Relay structures in a Lower Permian basement-involved extension system, East Greenland. Journal of Structural Geology 10, 3–8.

Lebel, D., Mountjoy, E.W., 1995. Numerical modelling of propagation and overlap of thrust faults, with application to the thrust-fold belt of central Alberta. Journal of Structural Geology 17, 631–646.

Mandal, N., Chattopadhyay, A., 1995. Modes of reverse-reactivation of domino-type normal faults: experimental and theoretical approach. Journal of Structural Geology 17, 1151–1163.

Marone, C., 1995. Fault zone strength and failure criteria. Geophysical Research Letters 22, 723–726.

Marshak, S., Wilkerson, M.S., Hsui, A.T., 1992. Generation of curved fold–thrust belts: insights from simple physical and analytical models. In: McClay, K.R. (Ed.), Thrust Tectonics. Chapman and Hall, pp. 83–92.

McClay, K.R., White, M.J., 1995. Analogue modelling of orthogonal and oblique rifting. Marine and Petroleum Geology 12, 137–151.

McLachlan, A.C., 1986. A Revised Interpretation of the Structures Within the Mesozoic of North-West Somerset. Unpublished M.Sc. thesis, Imperial College, London.

Morley, C.K., Nelson, R.A., Patton, T.L., Munn, S.G., 1990. Transfer zones in the East African Rift System and their relevance to hydrocarbon exploration in rifts. American Association of Petroleum Geologists Bulletin 74, 1234–1253.

Nemcok, M., Gayer, R., Miliorizos, M., 1995. Structural analysis of the inverted Bristol Channel Basin: implications of the geometry and timing of fracture porosity. In: Buchanan, J.G., Buchanan, P.G. (Eds.), Basin Inversion (special issue). Geological Society of London Special Publication 88, 355–392.

Nicholson, C., Seeber, L., Williams, P., Sykes, L.R., 1986. Seismicity and fault kinematics through the Eastern Transverse Ranges, California: block rotation, strike-slip faulting and low-angle thrusts. Journal of Geophysical Research 91, 4891–4908.

Palmer, C.P., 1972. The Lower Lias (Lower Jurassic) between

Watchet and Lilstock in north Somerset (UK). Newsletters on Stratigraphy 2, 1–30.

Peacock, D.C.P., 1996. Field examples of variations in fault patterns at different scales. Terra Nova 8, 361–371.

Peacock, D.C.P., Sanderson, D.J., 1991. Displacements, segment linkage and relay ramps in normal fault zones. Journal of Structural Geology 13, 721–733.

Peacock, D.C.P., Sanderson, D.J., 1992. Effects of layering and anisotropy on fault geometry. Journal of the Geological Society of London 149, 793–802.

Peacock, D.C.P., Sanderson, D.J., 1994a. Geometry and development of relay ramps in normal fault systems. American Association of Petroleum Geologists Bulletin 78, 146–165.

Peacock, D.C.P., Sanderson, D.J., 1994b. Strain and scaling of faults in the chalk at Flamborough Head, U.K. Journal of Structural Geology 16, 97–107.

Peacock, D.C.P., Sanderson, D.J., 1995. Strike-slip relay ramps. Journal of Structural Geology 17, 1351–1360.

Peacock, D.C.P., Zhang, X., 1994. Field examples and numerical modelling of oversteps and bends along normal faults in cross-section. Tectonophysics 234, 147–167.

Rawson, P.F., Wright, J.K., 1992. The Yorkshire Coast. Geologists' Association, London Geologists' Association Guide No. 34.

Roberts, A.M., Price, J.D., Olsen, T.S., 1990. Late Jurassic half-graben control on the siting and structure of hydrocarbon accumulations: UK/Norwegian Central Graben. In: Hardman, R.F.P., Brooks, J. (Eds.), Tectonic Events Responsible for Britain's Oil and Gas Reserves (special issue). Geological Society of London Special Publication 55, 229–257.

Roberts, D.G., 1989. Basin inversion in and around the British Isles. In: Cooper, M.A., Williams, G.D. (Eds.), Inversion Tectonics (special issue). Geological Society of London Special Publication 44, 131–152.

Sahimi, M., Arbabi, S., 1996. Scaling laws for fracture of heterogeneous materials and rock. Physical Review Letters 77, 3689–3692.

Sanderson, D.J., Marchini, W.R.D., 1984. Transpression. Journal of Structural Geology 6, 449–458.

Scott, D.R., Marone, C.J., Sammis, C.G., 1994. The apparent friction of granular fault gouge in sheared layers. Journal of Geophysical Research 99, 7231–7246.

Sibson, R.H., 1985. A note on fault reactivation. Journal of Structural Geology 7, 751–754.

Sibson, R.H., 1995. Selective fault reactivation during basin inversion: potential for fluid redistribution through fault-valve action. In: Buchanan, J.G., Buchanan, P.G. (Eds.), Basin Inversion (special issue). Geological Society of London Special Publication 88, 3–19.

Stark, C.P., Stark, J.A., 1991. Seismic fluids and percolation theory. Journal of Geophysical Research 96, 8417–8426.

Stauffer, D., Aharony, A., 1992. Introduction to Percolation Theory, 2nd ed. Taylor and Francis, London.

Thomas, D.W., Coward, M.P., 1995. Late Jurassic–Early Cretaceous inversion of the northern East Shetland Basin, northern North Sea. In: Buchanan, J.G., Buchanan, P.G. (Eds.), Basin Inversion (special issue). Geological Society of London Special Publication 88, 275–306.

Trudgill, B., Cartwright, J., 1994. Relay-ramp forms and normal-fault linkages, Canyonlands National Park, Utah. Geological Society of America Bulletin 106, 1143–1157.

Turcotte, D.L., 1995. Chaos, fractals and nonlinear phenomena in Earth Sciences. Reviews of Geophysics 33, 341–343.

Van Hoorn, B., 1987. The South Celtic Sea/Bristol Channel Basin: origin, deformation and inversion history. Tectonophysics 137, 309–334.

Walsh, J.J., Watterson, J., 1988. Analysis of the relationship between displacements and dimensions of faults. Journal of Structural Geology 10, 239–247.

Warrington, G., Scrivener, R.C., 1980. The Lyme Regis (1901) Borehole succession and its relationship to the Triassic sequence of the east Devon coast. Proceedings of the Ussher Society 5, 24–32.

Whittaker, A., Green, G.W., 1983. Geology of the County Around Weston-super-Mare. Geological Survey of Great Britain.

Williams, G.D., Powell, C.M., Cooper, M.A., 1989. Geometry and kinematics of inversion tectonics. In: Cooper, M.A., Williams, G.D. (Eds.), Inversion Tectonics (special issue). Geological Society of London Special Publication 44, 3–16.